Journal of Immunological Methods 453 (2018) 3–10

Contents lists available at ScienceDirect

Journal of Immunological Methods

journal homepage: www.elsevier.com/locate/jim

Research paper

Deep immune profiling by mass cytometry links human T and NK cell differentiation and cytotoxic molecule expression patterns

Bertram Bengsch [a,b], Takuya Ohtani [b,d], Ramin Sedaghat Herati [b,c], Niels Bovenschen [e], Kyong-Mi Chang [c,d], E. John Wherry [a,b,*]

[a] Department of Microbiology, University of Pennsylvania Perelman School Medicine, Philadelphia, PA 19104, USA
[b] Institute for Immunology, University of Pennsylvania Perelman School Medicine, Philadelphia, PA 19104, USA
[c] Department of Medicine, University of Pennsylvania Perelman School Medicine, Philadelphia, PA 19104, USA
[d] Corporal Michael J. Crescenz Department of Veterans Affairs Medical Center, Philadelphia, PA 19104, USA
[e] Department of Pathology and Laboratory of Translational Immunology, University Medical Center Utrecht, Utrecht 3584 CX, The Netherlands

ARTICLE INFO

Article history:
Received 29 July 2016
Received in revised form 15 February 2017
Accepted 16 March 2017
Available online 19 March 2017

Keywords:
Mass cytometry
T cell
NK cell
Cytotoxic
Granzymes and perforin
T cell differentiation

ABSTRACT

The elimination of infected or tumor cells by direct lysis is a key T and NK cell effector function. T and NK cells can kill target cells by coordinated secretion of cytotoxic granules containing one or both pore-forming proteins, perforin and granulysin and combinations of granzyme (Gzm) family effector proteases (in humans: Gzm A, B, K, M and H). Understanding the pattern of expression of cytotoxic molecules and the relationship to different states of T and NK cells may have direct relevance for immune responses in autoimmunity, infectious disease and cancer. Approaches capable of simultaneously evaluating expression of multiple cytotoxic molecules with detailed information on T and NK differentiation state, however, remain limited. Here, we established a high dimensional mass cytometry approach to comprehensively interrogate single cell proteomic expression of cytotoxic programs and lymphocyte differentiation. This assay identified a coordinated expression pattern of cytotoxic molecules linked to CD8 T cell differentiation stages. Coordinated high expression of perforin, granulysin, Gzm A, Gzm B and Gzm M was associated with markers of late effector memory differentiation and expression of chemokine receptor CX3CR1. However, classical gating and dimensionality reduction approaches also identified other discordant patterns of cytotoxic molecule expression in CD8 T cells, including reduced perforin, but high Gzm A, Gzm K and Gzm M expression. When applied to non-CD8 T cells, this assay identified different patterns of cytotoxic molecule co-expression by $CD56^{hi}$ versus $CD56^{dim}$ defined NK cell developmental stages; in CD4 T cells, low expression of cytotoxic molecules was found mainly in TH1 phenotype cells, but not in Tregs or T follicular helper cells (TFH). Thus, this comprehensive, single cell, proteomic assessment of cytotoxic protein co-expression patterns demonstrates specialized cytotoxic programs in T cells and NK cells linked to their differentiation stages. Such comprehensive cytotoxic profiling may identify distinct patterns of cytotoxic potential relevant for specific infections, autoimmunity or tumor settings.

1. Introduction

In response to infections or transformation, T and NK cells can directly kill target cells. This effector function can be exerted by the ligation of death receptors or by coordinated secretion of cytotoxic granules containing pore-forming proteins (perforin) and effector proteases (e.g., granzyme (Gzm) family, granulysin) (Voskoboinik et al., 2015). These granules are delivered to the interface of the cytotoxic lymphocyte and target cell where, upon release, perforin monomers insert into the target cell membrane and polymerize to form a pore. Granule contents including the effector protease enzymes are delivered through this pore and subsequently cleave key intracellular proteins to initiate a cascade of apoptotic and non-apoptotic cell death. Although Gzm B has been studied most extensively, multiple Gzms, (A, B, K, M and H) are expressed by human cytotoxic lymphocytes. While other functions of Gzms exist and there may be non-perforin mechanisms of Gzm uptake in target cells (Wensink et al., 2015), this coordinated cytotoxic molecule pathway likely represents the canonical cytotoxic mechanism used by CD8 T and NK cells to combat infected or transformed host cells.

Expression of perforin is critical for the killing capacity of T cells and has been linked to control of HIV (Harari et al., 2009; Hersperger et al., 2010). Virus-specific T cells targeting persistent, yet controlled CMV

* Corresponding author at: Department of Microbiology, University of Pennsylvania Perelman School Medicine, Philadelphia, PA 19104, USA.
E-mail address: wherry@mail.med.upenn.edu (E.J. Wherry).

http://dx.doi.org/10.1016/j.jim.2017.03.009

infection express high levels of perforin and have high killing capacity (Harari et al., 2009). In contrast, T cells in highly viremic HIV- or HCV-infected patients express low levels of perforin, suggesting that absence of full cytotoxic capacity favors viral persistence (Appay et al., 2000; Zhang et al., 2003; Hersperger et al., 2010; Jo et al., 2012). Granulysin, a member of the saposin-like protein family, can facilitate Gzm delivery and cell death through bacterial walls (Walch et al., 2014), likely explaining its prominent role in antifungal and anti-tuberculosis responses (Stenger et al., 1998; Ma et al., 2002). Thus, T cells can employ distinct cytotoxic mechanisms to combat differing pathogens.

In addition to the role of cytotoxic cells in infection, the historical appreciation of a requirement for perforin- and cytotoxic molecule mediated killing for the elimination of cancer cells (Kagi et al., 1994; Voskoboinik et al., 2015) recently received renewed attention by the identification of a cytotoxic signature associated with outcome in cancer (Rooney et al., 2015). These studies used large genome-scale analyses of solid tissue biopsies to reveal a link between the presence of a cytolytic signature, neoepitope load, immunoediting and disease progression across various cancers (Rooney et al., 2015). Indeed, the highest expression of *GZMA* and *PRF1* in tumor biopsies was linked to favorable survival (Rooney et al., 2015). However, it remains currently unclear whether distinct cytotoxic cell types and/or specific patterns of cytotoxic molecule expression are directly responsible for the prolonged survival. For example, it remains unclear whether these signatures stem from cytotoxic CD8 T cells, cytotoxic CD4 T cells, NK cells or additional cell types. Further, how expression of the different components of the lytic machinery in cytotoxic cells is coordinated remains poorly understood.

The cytotoxic potential of CD8 T cells is low in naïve T cells and induced during priming and differentiation to effector cells. Whereas all Gzms are thought to be able to induce cell death based on high-dose in vitro killing studies, in vivo functions of distinct Gzms may differ (Joeckel and Bird, 2014). For example, different Gzms have been reported to be involved in degrading extracellular matrix, modulating proinflammatory cytokines (Wensink et al., 2015), or exerting direct antiviral effects (van Domselaar et al., 2010), suggesting that Gzm family members may have evolved for specialized functional roles. In this context, it is interesting to note that T cells may also express different combinations of Gzms. For example, while Gzm expression is lacking in naïve T cells, the majority of memory T cells co-express either Gzm A and Gzm K or Gzm A and Gzm B, with a low number of CD8 T cells simultaneously expressing Gzm A, Gzm B and Gzm K (Bratke et al., 2005). In some settings, the co-expression patterns of these Gzms were linked to the expression of memory or effector markers of CD8 T cells, (Bratke et al., 2005; Harari et al., 2009). In other studies, expression of Gzm M and granulysin was associated with antigen-experienced differentiated T cell subsets (Bruns et al., 2009; de Koning et al., 2010). In addition to studies analyzing the relationship of differentiation markers to cytotoxic molecule expression, expression of the fractalkine receptor CX3CR1 was recently described as a useful marker of cytotoxic memory T cells in humans (Bottcher et al., 2015). However, in that study, analysis of protein expression of cytotoxic molecules was limited to Gzm B and perforin. These reports suggest that T cells may co-express different sets of cytotoxic molecules and that these patterns may reflect distinct specialized cytotoxic programs related to the state of T cell differentiation. However, in these studies, use of conventional flow cytometry limited the number of cytotoxic and differentiation molecules that could be simultaneously examined, and prevented comprehensive analysis of cytotoxic molecule and differentiation marker expression patterns. Further, it remains unclear if cytotoxic programs are shared across different lineages of cytotoxic cells (e.g., NK cells, CD8 and CD4 T cells), and how cytotoxic programs influence disease.

Addressing these questions requires the concurrent analysis of multiple cytotoxic molecules, lineage and differentiation markers. The use of mass cytometry allows the simultaneous analysis of >40 proteins on single cells providing high-dimensional data necessary for insights into complex cellular expression patterns (Spitzer and Nolan, 2016). In this work, we developed a mass cytometry panel suitable for the analysis of combinatorial cytotoxic molecule expression across NK and T cell lineages. The comprehensive, single cell, proteomic assessment of cytotoxic protein co-expression patterns demonstrates specialized cytotoxic programs in T cells and NK cells linked to their differentiation stages. Cytotoxic profiling has implications for the understanding of T cell function in infection, autoimmunity and tumor immunology.

2. Methods

2.1. Reagents

Mass cytometry antibodies were obtained as pre-conjugated metal-tagged antibodies (abs) from Fluidigm or generated in-house by conjugating unlabeled purified abs to isotope-loaded polymers using MAXPAR kits (Fluidigm). Based on titration performance, antibodies were diluted in antibody stabilization buffer (Candor Bioscience). A detailed list of the antibodies used in this study is provided in Table 1. Antibody staining performance for Gzm H was not satisfactory and hence was not interrogated in detail. ^{113}In, ^{115}In and ^{139}La isotopes not available through Fluidigm were obtained from Trace Sciences, Inc. For viability discrimination, maleimido-mono-amine-DOTA (Macrocyclics) was dissolved in MAXPAR L-Buffer (Fluidigm) and mixed with ^{139}La (L/D-139) for a 0.5 mM final concentration.

Table 1
Antibodies and panel information.

Isotope channel	Antibody/reagent name	Clone	Source	Category
89 Y	CD45	HI30	Fluidigm	Lineage
113 In	CD45RO	UCHL1	BD	Differentiation
115 In	CD57	TB01	Ebioscience	Differentiation
139 La	L/D MM-DOTA		In-house	Viability
140 etc.	Beads		Fluidigm	QC
141 Pr	CD3	UCHT1	Biolegend	Lineage
142 Nd				
143 Nd	CD4	RPA-T4	Biolegend	Lineage
144 Nd				
145 Nd	Granulysin	DH2	Biolegend	Cytotox
146 Nd	CD8	RPA-T8	Biolegend	Lineage
147 Sm	CD45RA	H100	BD	Differentiation
148 Nd	CD95	DX2	Biolegend	Differentiation
149 Sm	CD14	M5E2	Biolegend	Lineage
150 Nd	CD127	HIL-7R-M21	BD	Differentiation
151 Eu				
152 Sm	Granzyme B	CLB-GB11	Novus	Cytotox
153 Eu				
154 Sm	Granzyme K	GM6C3	Santa Cruz	Cytotox
155 Gd	CD27	L128	Fluidigm	Differentiation
156 Gd				
158 Gd	PD-1	EH12.2H7	Fluidigm	IR
159 Tb	CCR7	G043H7	Fluidigm	Differentiation
160 Gd	Tbet	4B10	Fluidigm	Differentiation
161 Dy	CD28	CD28.2	Biolegend	Differentiation
162 Dy	Foxp3	PCH101	Fluidigm	Treg
163 Dy				
164 Dy				
165 Ho	Eomes	WD1928	Ebioscience	Differentiation
166 Er	Perforin	B-D48	Abcam	Cytotox
167 Er				
168 Er	CX3CR1	2A9-1	Biolegend	Cytotox
169 Tm	TIGIT	MBSA43	Ebioscience	IR
170 Er	CXCR5	RF8B2	BD	TFH
171 Yb	2B4	C1.7	Biolegend	IR
172 Yb	Granzyme A	CD9	Biolegend	Cytotox
173 Yb	Granzyme M	4B2G4	Bovenschen	Cytotox
174 Yb				
175 Lu	Granzyme H	ARP42686_T100	Aviva pAb	failed QC
176 Yb	CD56	HCD56	Fluidigm	Lineage
191/193	Iridium			DNA
209 Bi	CD16	3G8	Fluidigm	Lineage

2.2. Staining

PBMCs from healthy donors were obtained by an experienced phlebotomist after written informed consent in Lithium-Heparin coated tubes. PBMCs were isolated via ficoll-histopaque density gradient centrifugation (Ficoll-Paque PLUS, GE Healthcare Life Sciences). Briefly, blood was diluted 1:1 with PBS and 35 ml of diluted blood was overlaid on 15 ml ficoll in 50 ml tubes prior to centrifugation for 20 min at RT (2000 rpm/805 rcf, acceleration & brake setting: 0 on Eppendorf R 5810 series centrifuge). Lymphocyte layer was collected, transferred to a new 50 ml tube, washed in PBS and pelleted (5 min, RT, 1500 rpm, acceleration & brake setting: 9, settings also used in the following steps). Supernatant was discarded and cells were counted using an automated cell counter (Invitrogen Countess). 4×10^6 PBMC/subject/well were transferred into 96-well U-bottom tissue culture plates. Single-cell suspensions were pelleted, and incubated with 20 μM L/D-139 (50 μl staining volume) for 10 min at room temperature (RT) for live/dead discrimination. Cells were washed in staining buffer and resuspended in surface antibody cocktail (adjusted to 50 μl final volume with staining buffer: PBS (without Ca^{2+} and Mg^{2+}) with 1% FBS), incubated for 30 min at RT, washed twice in staining buffer, fixed and permeabilized in 50 μl Foxp3 Fixation/Permeabilization working solution (FoxP3 staining buffer set, eBioscience), and stained intracellularly for 60 min at RT (5 min, 4C, 1800 rpm, centrifuge settings used after permeabilization). Cells were further washed twice with 1× permeabilization buffer (Ebioscience) before fixation in 1.6% PFA solution (Electron Microscopy Sciences) containing 125 nM Iridium (Fluidigm) overnight at 4C. Prior to data acquisition on CyTOF2 (Fluidigm), cells were washed twice in PBS (without Ca^{2+} and Mg^{2+}) and once in deionized H_2O.

2.3. Data acquisition and analysis

Samples were acquired at a CyTOF2 (Fluidigm) with bead-based normalization of CyTOF data by using Nolan lab normalizer available through https://github.com/nolanlab/bead-normalization/releases. Bead data events were removed during export. FCS files were further analyzed by FlowJo v10 (TreeStar) and ViSNE (Cytobank). Statistical evaluation was performed using Graphpad Prism.

3. Results

3.1. Lymphocyte identification and T and NK cell differentiation states

We developed a mass cytometry panel to comprehensively interrogate cytotoxic molecule expression patterns, their relationship to T and NK cell lineages and the connection between T and NK differentiation stages and novel combinatorial patterns of cytotoxic molecule expression on a single-cell level (Table 1), and applied this approach to the analysis of PBMC from a cohort of healthy individuals. Live CD4 T cell, CD8 T cells and NK cells were identified by first gating on DNA-Intercalator positive singlet cells, low intensities of viability

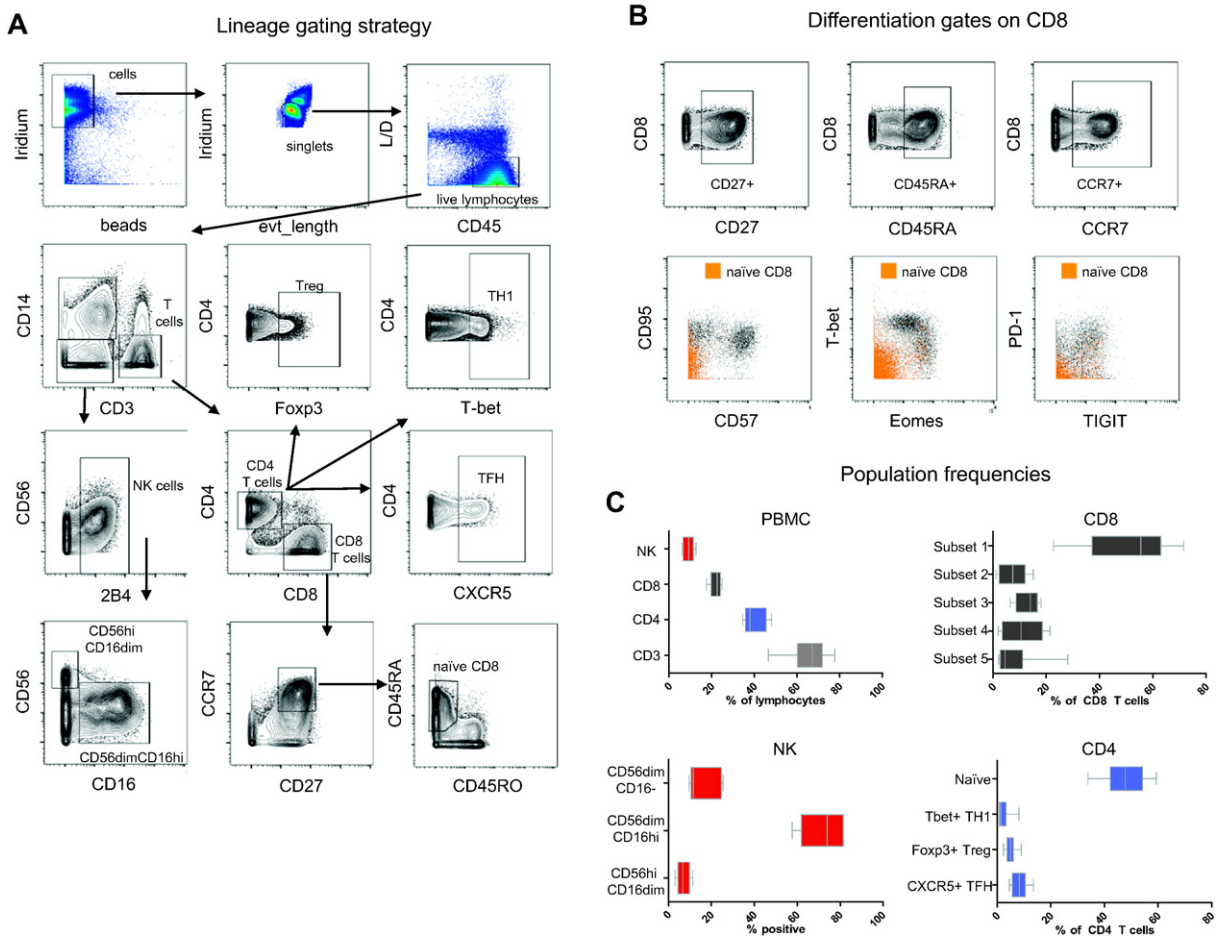

Fig. 1. Lineage gating PBMC from healthy donors were stained with the panel outlined in Table 1 and analyzed by mass cytometry. (A) Representative example of the gating strategy used to identify lymphocyte lineages and subpopulations. (B) (upper) Representative examples of the gates used to identify naïve T cells (positive for CD27, CD45RA and CCR7). (lower) overlay plot of CD27 + CD45RA + CCR7 + naïve phenotype cells (orange) over total CD8 cells, indicating little expression of markers associated with non-naïve T cells (CD95, CD57, T-bet, Eomes, PD-1 and TIGIT). (C) Healthy donors were analyzed for T cell and NK cell populations. Frequencies are displayed by box and whiskers plots with 5–95% interval.

discriminant dye and then examining lineage marker expression (Fig. 1A). We also identified T follicular helper-like cells (TFH) expressing CXCR5 +, regulatory T cells (Treg) based on Foxp3 expression, TH_1 cells based on T-bet expression and naïve T cells based on CCR7, CD27, CD45RA (Fig. 1A, B).

CD8 T cell populations were identified and distinguished into 5 differentiation subsets based on CD27, CD45RA and CCR7 expression (CD27 + CCR7 + CD45RA + subset 1 ➔ naïve; CD27 + CCR7 + CD45RA − subset 2 ➔ early differentiated or TCM; CD27 + CCR7 − CD45RA − subset 3 ➔ intermediate differentiated; CD27 − CCR7 − CD45RA − subset 4 ➔ advanced differentiated; CD27 − CCR7 − CD45RA + subset 5 ➔ late differentiated or TEMRA). We validated that this combination of markers identified naïve phenotype CD8 T cells that were low in expression of differentiation markers CD57, CD95, transcription factors T-bet and Eomes, and inhibitory receptors PD-1 and TIGIT (Fig. 1B). This strategy of segregating human CD8 T cells into these 5 subsets has been applied often to the study of virus-specific CD8 T cells and revealed insights into hepatitis B virus (HBV)-, hepatitis C virus (HCV)- and human immunodeficiency virus (HIV)-specific CD8 T cell differentiation (Sauce et al., 2007; Appay et al., 2008; Bengsch et al., 2010; Bengsch et al., 2014) and provides a framework for the analysis below. We also evaluated the abundance of CD4 T cell subpopulations, naïve and non-naïve CD8 T cells and NK cells in PBMCs from our cohort of healthy individuals. As shown in Fig. 1C, we observed a distribution of lymphocyte subpopulations typical of healthy individuals, with a predominance of naïve phenotype (subset 1) CD8 and CD4 T cells and a CD4:CD8 ratio of ~2:1. In sum, using 19 mass cytometry channels, we have created a backbone panel of lineage and differentiation markers needed for a detailed analysis of CD4, CD8 and NK cells and their differentiation stages that still allows addition of >20 other markers to further interrogate other features of lymphocyte biology.

3.2. Distinct expression patterns of cytotoxic molecules in T cell and NK cell subpopulations

We next evaluated the expression of cytotoxic molecules in CD8 and CD4 T cells and NK cells. Representative staining patterns for Gzm A, B, K and M, granulysin and perforin on CD8 T cells are shown in Fig. 2A. In general, expression of cytotoxic proteins was highest in NK cells, followed by CD8 T cells and lowest in CD4 T cells (Fig. 2B). In fact, among the analyzed CD4 populations, only TH_1 cells displayed expression of cytotoxic molecules, with highest expression observed for Gzm A (median:50%), followed by Gzm B, Gzm M and perforin (30–40%), with lower expression of Gzm K and granulysin (20% versus 10%). Interestingly, among NK cells, $CD56^{hi}$ and $CD56^{dim}$ CD16 + NK cells showed clearly different cytotoxic molecule expression patterns. $CD56^{hi}$ NK cells had low Gzm B, but high Gzm K expression, whereas the $CD56^{dim}$ CD16 + NK cell subset expressed high Gzm B but lacked Gzm K (Fig. 2B). Moreover, although the frequency of cells expressing detectable perforin was similar in both populations, the $CD56^{hi}$ NK subset expressed lower amounts of perforin compared to $CD56^{dim}$ CD16 + NK cells (Fig. 2B). These results implicate differential use of cytotoxic molecules across T and NK lineages.

3.3. Relationship of cytotoxic programs to CD8 T cell differentiation stages

We next examined the expression pattern of cytotoxic molecules in CD8 T cells relative to T cell differentiation stages defined by CD27, CCR7 and CD45RA (Fig. 3A). Consistent with previous reports, there was little

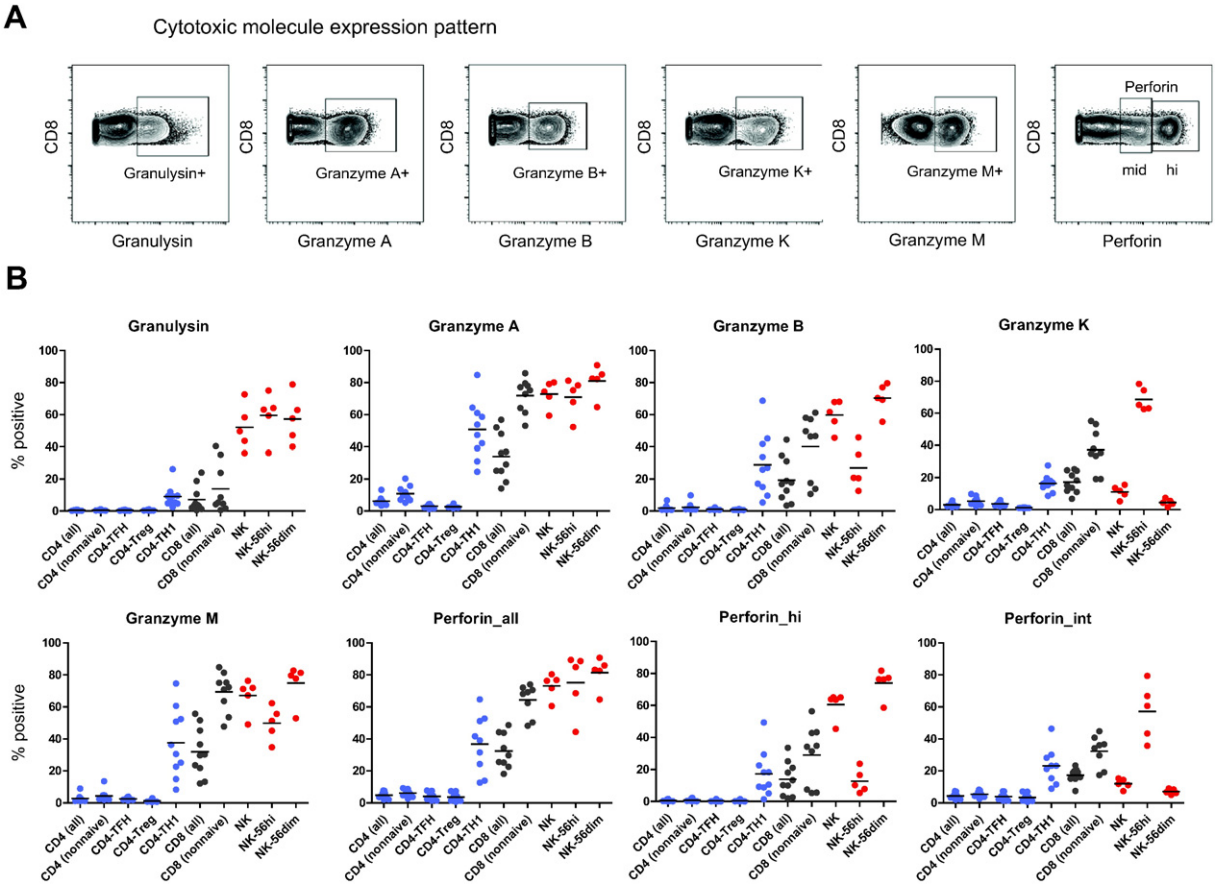

Fig. 2. Cytotoxic molecule expression on T and NK cells (A) Representative example of the gating strategy used to identify expression of cytotoxic molecules. Example is gated on CD8 T cells. (B) Scattered dot plots indicating frequency of cytotoxic molecule expression by T cell and NK cell subpopulations in the peripheral blood (population colors: CD4-blue, CD8-black, NK-red).

to no expression of cytotoxic molecules in naïve T cells (subset 1) (Fig. 3B). By contrast, 20–60% of early differentiated T cells (subset 2), expressed Gzm A, Gzm K, Gzm M and intermediate levels of perforin (perforin^{int}), with minimal expression of Gzm B, granulysin or high-levels of perforin (perforin^{hi}). Of note, Gzm B, granulysin and perforin^{hi} expression continued to increase as differentiation status advanced, reaching the highest levels up to 90% in late differentiated T cells (subset 5). The accumulation of Gzm B, granulysin and perforin expression as T cells differentiated to effector memory cells is in line with greater cytotoxicity observed in late differentiated effectors compared to early differentiated central memory or naïve CD8 T cells (Harari et al., 2009). Close to 100% of T cells in intermediate to late differentiation stages expressed Gzm A and M, suggesting that induction of Gzm A and M is an event that occurs early after T cell activation and is maintained throughout further T cell differentiation, but also stably maintained in these less differentiated subsets. In contrast, for Gzm K, we observed peak expression in T cells in the intermediate differentiation compartment, lower frequencies in early and advanced differentiated subsets, and lack of expression in late differentiated T cells. Interestingly, a similar expression pattern was observed for perforin^{int} T cells, that were of highest frequency in the intermediate stages of differentiation. Taken together, our results reveal several distinct cytotoxic molecule expression patterns linked to T cell differentiation stages.

CX3CR1 expression has been linked to the cytotoxic program of CD8 T cells and was proposed to allow functional classification between memory CD8 T cells with cytotoxic effector function and those with proliferative capacity (Bottcher et al., 2015). The maintenance of cytotoxic effector cells in an intermediate differentiated precursor pool may be key to the control of persistent infections (Chu et al., 2016). We therefore examined the expression of CX3CR1 on CD8 T cell differentiation subsets. CX3CR1 expression was nearly undetectable on naïve and early differentiated T cells. In contrast, CX3CR1 expression was low on intermediate differentiated cells and highest in late differentiated cells (Fig. 3B). Thus, the pattern of CX3CR1 expression resembled that of Gzm B and perforin^{hi}, in agreement with the notion that CX3CR1 is linked to cells with a cytotoxic program.

3.4. Coexpression patterns of cytotoxic molecules

Our previous analyses indicated that different patterns of cytotoxic molecule expression related to T cell differentiation. However, on a single cell level, the cellular expression of cytotoxic molecules might not necessarily follow the global CD8 differentiation patterns. As traditional analysis presented above did not dissect this issue, we set out to examine distinct single cell co-expression patterns of cytotoxic molecules in CD8 T cells. Bivariate expression plots of individual cytotoxic proteins shown in Fig. 4A supported the notion of heterogeneity of granzyme coexpression patterns at the single cell level. Due to the complexity of representing multiple (>2) cytotoxic molecule co-expression patterns on a single cell level, we employed a dimensionality reduction technique using t stochastic neighborhood embedding (tSNE) to map the high dimensional data into two dimensions by viSNE (Amir el et al., 2013). This approach reveals the heterogeneity of single-cell cytotoxic molecule expression patterns while aiming to retain the high-dimensional data structure but is not confounded by a priori knowledge about cytotoxic molecule expression, coexpression of differentiation markers or gating strategy. We therefore used it to derive a 2-dimensional representation of all high-dimensional cytotoxic molecule expression phenotypes of CD8 T cells, allowing an easier assessment of the relatedness of different T cells populations based on their cytotoxic marker profile as indicated by their proximity in the tSNE-based representation. As shown in Fig. 4B, this analysis identifies three major groups of CD8 T cells: i) cells

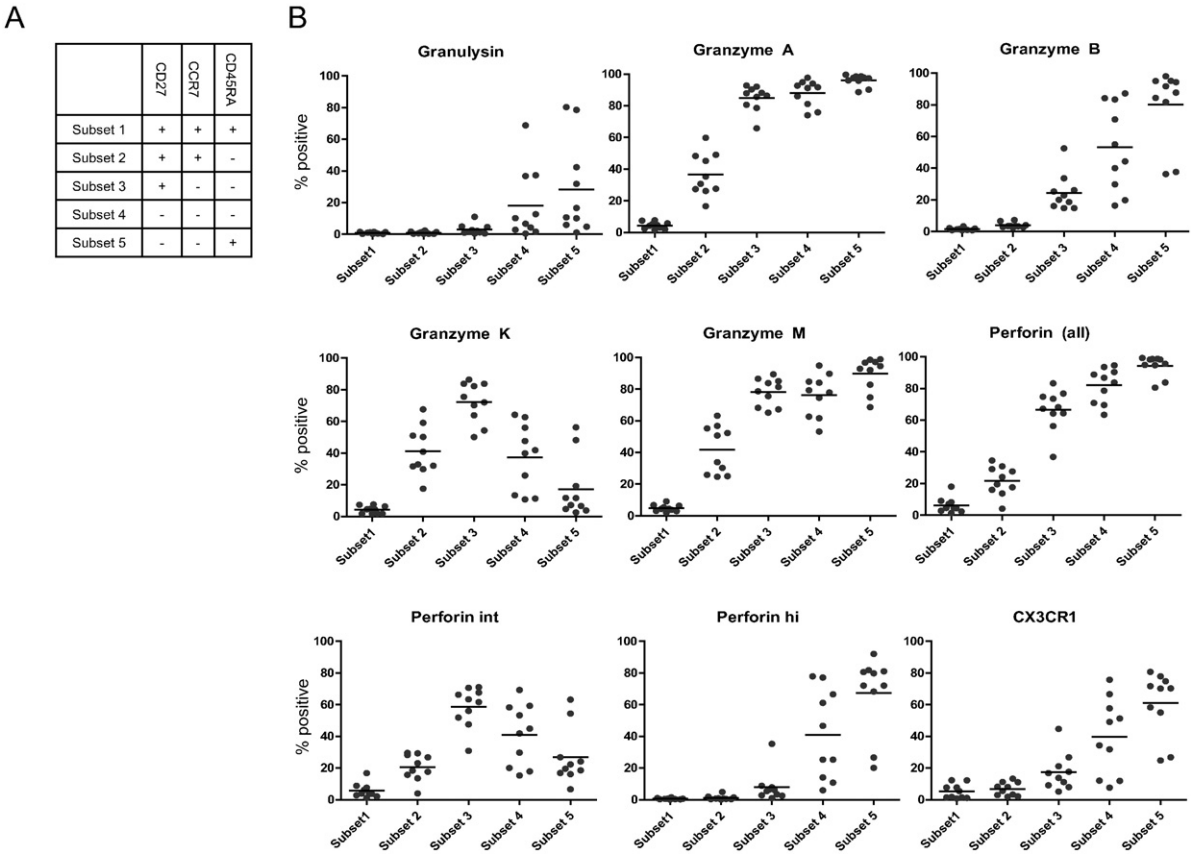

Fig. 3. Cytotoxic molecule expression patterns are linked to CD8 T cell differentiation (A) CD8 T cell differentiation subsets were distinguished using a classification based on CD27, CD45RA and CCR7. (B) Scattered dot plots indicating frequency of cytotoxic molecule expression by CD8 T cell differentiation populations in the peripheral blood reveals distinct patterns of cytotoxic molecule expression along developmental trajectories.

with low to absent cytotoxic molecule expression; ii) cells with high Gzm A, B, M co-expression; and iii) cells with Gzm A, M and K co-expression. Of note, these larger clusters could be further subdivided based on granulysin, perforin and CX3CR1 expression. In addition, these clusters correlated well with the expression of CD28, CD57 and CD95, which had not been used to compute the dimensionality reduction.

We next asked whether these co-expression patterns were shared across cytotoxic lineages. To compare the cytotoxic map of CD8 T cells to that of NK cells, we generated a novel tSNE analysis based on the cytotoxic molecule expression data from the CD8 T cell and NK cell populations. We observed similar groups of cells with cytotoxic co-expression programs including cells with low to absent cytotoxic molecule expression, cells with high Gzm A, B, M coexpression and cells with Gzm A, M and K coexpression (Fig. 4C). However, in addition to the previous analysis based solely on CD8 T cells, we observed further heterogeneity among the cells expressing no cytotoxic molecules. Comparison of the cytotoxic map of CD8 T cells and the NK populations indicated that NK cells expressed a less diverse program of cytotoxic markers compared to CD8 T cells (Fig. 4D). Of note, the cytotoxic program of CD56^{dim} CD16+ NK cells largely overlapped with that of perforin^{hi} CD8 T cells, while CD56^{hi} NK cells mapped to a low Gzm B, high Gzm K and intermediate perforin expression pattern (Fig. 4E). Thus, both classical and algorithm-guided dimension reduction analysis indicate two divergent major programs of cytotoxic molecule co-expression that are conserved between T cells and NK cells. These approaches also revealed additional complexity in these patterns that may be relevant when evaluating human disease states.

4. Discussion

Here, we established a mass cytometry approach to comprehensively measure single cell proteomic expression of cytotoxic programs

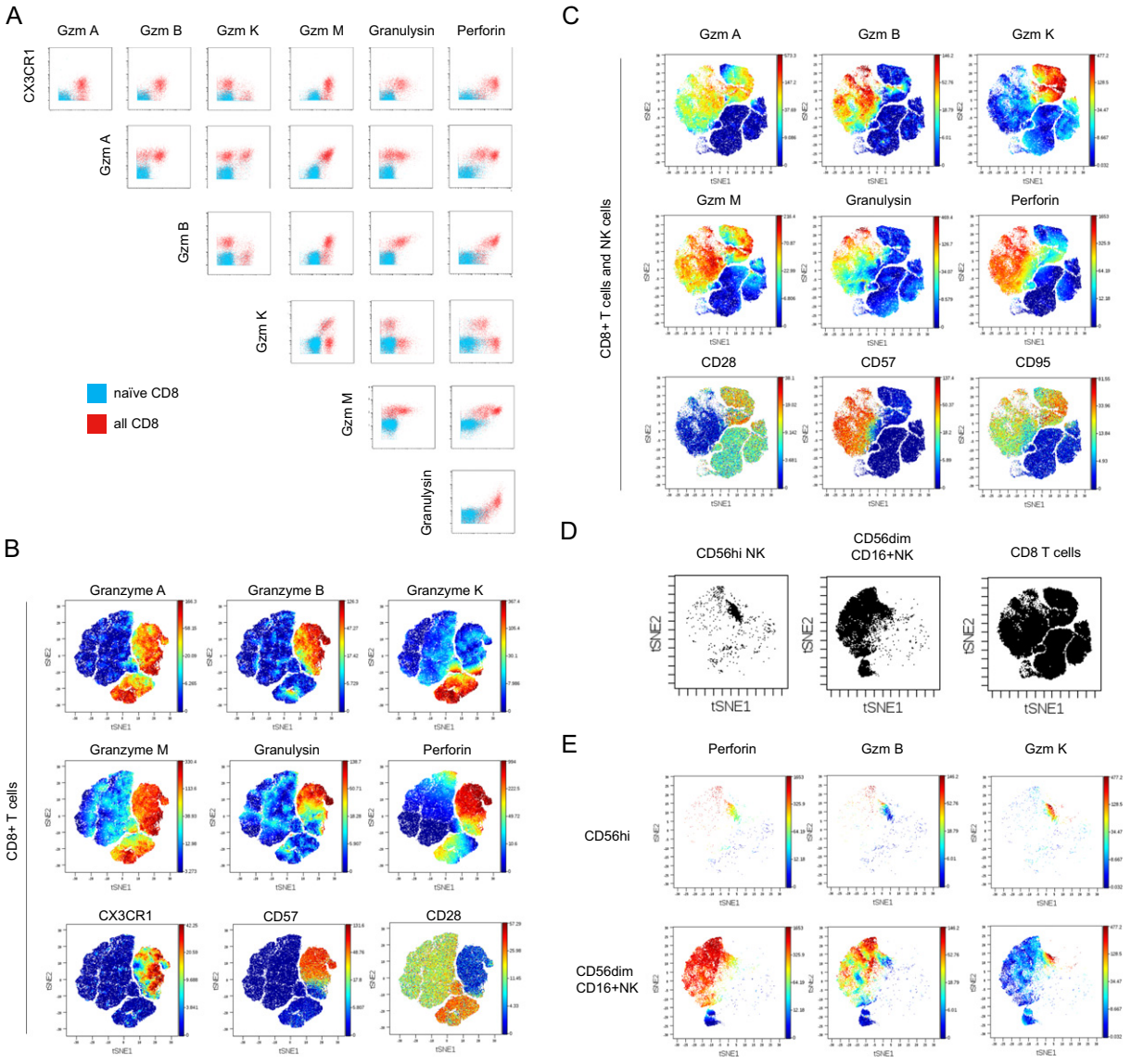

Fig. 4. Distinct coexpression patterns of cytotoxic molecules partly overlap across lineages (A) Representative bivariate coexpression plots of cytotoxic molecules analyzed. CD27 + CD45RA + CCR7+ naïve phenotype cells (blue) were overlaid on total CD8 T cells (red). (B) tSNE-based dimension reduction with viSNE was performed on CD8 T cells using the high-dimensional information of cytotoxic molecule channels. Expression of cytotoxic molecules is presented as heatmap overlay over cells arranged by their tSNE coordinates to illustrate high-dimensional population features in two dimensions (upper two rows). This approach reveals populations of CD8 T cells with distinct coexpression patterns that are linked to the expression of CX3CR1, CD57 and CD28 (not used for the viSNE analysis). An extended analysis in (C) was performed on CD8 and NK cells to facilitate cross-comparison. (D) Populations of CD56^{hi} and CD56^{dim} CD16+ cells were analyzed by the tSNE dimensions, revealing distinct, shared, but less diverse cytotoxic phenotypes compared to CD8 T cells. (E) Overlay heatmaps of Perforin, Gzm B and Gzm K reveal key differences between CD56^{hi} and CD56^{dim} CD16+ NK cells.

among stages of T cell differentiation. We also show that this assay can be easily modified to profile other immune lineages (e.g., NK cells) given the ability to accommodate additional markers in the CyTOF panels. This assay identifies T cells expressing high levels of perforin, granulysin, Gzm A, B and M that have late effector memory differentiation phenotypes and expression of CX3CR1. However, expression of discordant cytotoxic programs, including reduced perforin but high Gzm A, K and M coexpression, were also readily identified by classical gating or dimension-reduction techniques. Further, our approach provided additional insights as expression levels of cytotoxic molecules were compared across lymphocyte lineages, such as TH_1 cells or NK cells. For example, our data indicate that the expression of cytotoxic molecules in CD4 T cells occurs only in the subset expressing T-bet, consistent with the role for T-bet in driving cytotoxic programs (Cruz-Guilloty et al., 2009), but also suggesting that cytotoxic CD4 T cells represent only a small population of T helper cells. Interestingly, our analyses also identified shared cytotoxic expression programs between CD8 T cells and NK cells, although NK cells were more restricted in co-expression patterns of cytotoxic molecules, possibly reflecting a more directed specialization towards killing capacity of NK cells. Analysis of cytotoxic molecule expression related to differentiation stages identified patterns such as the Gzm K and perforin^{int} phenotype peaking in intermediate differentiated cells, or the Gzm B and perforin^{hi} phenotype linked to late stages of differentiation. In agreement with previous reports, the link between these phenotypes and the linear differentiation model suggested a connection between the developmental history of CD8 T cells and their expression of cytotoxic molecules. Thus, our high-content mass cytometry analysis confirms and extends previous reports that implicated the expression of cytotoxic molecules to developmental trajectories of T cell differentiation.

There were also major differences in the cytotoxic expression patterns between CD56^{hi} and CD56^{dim} CD16+ NK cells, with CD56^{hi} NK cells expressing high levels of Gzm K, low levels of Gzm B and intermediate perforin (resembling the pattern for intermediate differentiated CD8 T cells) and CD56^{dim} CD16+ cells expressing high Gzm B and perforin but little Gzm K, sharing the cytotoxic program invoked in advanced and late CD8 T cell differentiation. Since CD56^{hi} NK cells have been perceived as the precursor population of CD56^{dim} cells (Yu et al., 2013), these data support the notion that cytotoxic expression patterns are conserved across lymphocyte lineages in a developmentally controlled manner.

Our panel uses a core of 25 channels including markers suitable for the delineation of NK and CD4 and CD8 T cell populations and their differentiation states with comprehensive coverage of cytotoxic molecules expression. To our knowledge, this assay represents the most comprehensive cytotoxic molecule single-cell co-expression assay applicable to human specimens published to date. Nevertheless, further development of reagents suitable to detect additional molecules involved in the cytotoxic response may reveal additional complexity. Conveniently, our approach allows for further customization in the remaining ~20 unused channels commonly available in mass cytometry, providing ample opportunity to extend the panel towards the investigation of additional proteins and cell populations.

In sum, our profiling demonstrates specialized cytotoxic programs in T cells linked to their differentiation stages. Cytotoxic profiling has important implications for the understanding of T cell function in infection, autoimmunity and tumor immunology.

Acknowledgments

We thank the Institute for Immunology (University of Pennsylvania) and the Corporal Michael J. Crescenz Department of Veterans Affairs Medical Center, Philadelphia for supporting the CyTOF core. BB. was supported by German Research Foundation fellowship BE5496/1-1. KMC was supported by the Corporal Michael J. Crescenz Department of Veterans Affairs Medical Center, UO-1DK082866 and VA 5I01BX000649. This work was funded by the National Institutes of Health grants AI105343, AI082630, AI117950 to EJW. This research was also supported by the Parker Institute for Cancer Immunotherapy. EJW has a patent licensing agreement on the PD-1 pathway. The authors declare no additional conflicts of interest.

References

Amir el, A.D., Davis, K.L., Tadmor, M.D., Simonds, E.F., Levine, J.H., Bendall, S.C., Shenfeld, D.K., Krishnaswamy, S., Nolan, G.P., Pe'er, D., 2013. viSNE enables visualization of high dimensional single-cell data and reveals phenotypic heterogeneity of leukemia. Nat. Biotechnol. 31, 545–552.

Appay, V., Nixon, D.F., Donahoe, S.M., Gillespie, G.M., Dong, T., King, A., Ogg, G.S., Spiegel, H.M., Conlon, C., Spina, C.A., Havlir, D.V., Richman, D.D., Waters, A., Easterbrook, P., McMichael, A.J., Rowland-Jones, S.L., 2000. HIV-specific CD8(+) T cells produce antiviral cytokines but are impaired in cytolytic function. J. Exp. Med. 192, 63–75.

Appay, V., van Lier, R.A., Sallusto, F., Roederer, M., 2008. Phenotype and function of human T lymphocyte subsets: consensus and issues. Cytometry A 73, 975–983.

Bengsch, B., Seigel, B., Ruhl, M., Timm, J., Kuntz, M., Blum, H.E., Pircher, H., Thimme, R., 2010. Coexpression of PD-1, 2B4, CD160 and KLRG1 on exhausted HCV-specific CD8+ T cells is linked to antigen recognition and T cell differentiation. PLoS Pathog. 6, e1000947.

Bengsch, B., Martin, B., Thimme, R., 2014. Restoration of HBV-specific CD8+ T cell function by PD-1 blockade in inactive carrier patients is linked to T cell differentiation. J. Hepatol. 61, 1212–1219.

Bottcher, J.P., Beyer, M., Meissner, F., Abdullah, Z., Sander, J., Hochst, B., Eickhoff, S., Rieckmann, J.C., Russo, C., Bauer, T., Flecken, T., Giesen, D., Engel, D., Jung, S., Busch, D.H., Protzer, U., Thimme, R., Mann, M., Kurts, C., Schultze, J.L., Kastenmuller, W., Knolle, P.A., 2015. Functional classification of memory CD8(+) T cells by CX3CR1 expression. Nat. Commun. 6, 8306.

Bratke, K., Kuepper, M., Bade, B., Virchow Jr., J.C., Luttmann, W., 2005. Differential expression of human granzymes A, B, and K in natural killer cells and during CD8+ T cell differentiation in peripheral blood. Eur. J. Immunol. 35, 2608–2616.

Bruns, H., Meinken, C., Schauenberg, P., Harter, G., Kern, P., Modlin, R.L., Antoni, C., Stenger, S., 2009. Anti-TNF immunotherapy reduces CD8+ T cell-mediated antimicrobial activity against *Mycobacterium tuberculosis* in humans. J. Clin. Invest. 119, 1167–1177.

Chu, H.H., Chan, S.W., Gosling, J.P., Blanchard, N., Tsitsiklis, A., Lythe, G., Shastri, N., Molina-Paris, C., Robey, E.A., 2016. Continuous effector CD8(+) T cell production in a controlled persistent infection is sustained by a proliferative intermediate population. Immunity 45, 159–171.

Cruz-Guilloty, F., Pipkin, M.E., Djuretic, I.M., Levanon, D., Lotem, J., Lichtenheld, M.G., Groner, Y., Rao, A., 2009. Runx3 and T-box proteins cooperate to establish the transcriptional program of effector CTLs. J. Exp. Med. 206, 51–59.

van Domselaar, R., Philippen, L.E., Quadir, R., Wiertz, E.J., Kummer, J.A., Bovenschen, N., 2010. Noncytotoxic inhibition of cytomegalovirus replication through NK cell protease granzyme M-mediated cleavage of viral phosphoprotein 71. J. Immunol. 185, 7605–7613.

Harari, A., Bellutti Enders, F., Cellerai, C., Bart, P.A., Pantaleo, G., 2009. Distinct profiles of cytotoxic granules in memory CD8 T cells correlate with function, differentiation stage, and antigen exposure. J. Virol. 83, 2862–2871.

Hersperger, A.R., Pereyra, F., Nason, M., Demers, K., Sheth, P., Shin, L.Y., Kovacs, C.M., Rodriguez, B., Sieg, S.F., Teixeira-Johnson, L., Gudonis, D., Goepfert, P.A., Lederman, M.M., Frank, I., Makedonas, G., Kaul, R., Walker, B.D., Betts, M.R., 2010. Perforin expression directly ex vivo by HIV-specific CD8 T-cells is a correlate of HIV elite control. PLoS Pathog. 6, e1000917.

Jo, J., Bengsch, B., Seigel, B., Rau, S.J., Schmidt, J., Bisse, E., Aichele, P., Aichele, U., Joeckel, L., Royer, C., Sa Ferreira, K., Borner, C., Baumert, T.F., Blum, H.E., Lohmann, V., Fischer, R., Thimme, R., 2012. Low perforin expression of early differentiated HCV-specific CD8+ T cells limits their hepatotoxic potential. J. Hepatol. 57, 9–16.

Joeckel, L.T., Bird, P.I., 2014. Are all granzymes cytotoxic in vivo? Biol. Chem. 395, 181–202.

Kagi, D., Ledermann, B., Burki, K., Seiler, P., Odermatt, B., Olsen, K.J., Podack, E.R., Zinkernagel, R.M., Hengartner, H., 1994. Cytotoxicity mediated by T cells and natural killer cells is greatly impaired in perforin-deficient mice. Nature 369, 31–37.

de Koning, P.J., Tesselaar, K., Bovenschen, N., Colak, S., Quadir, R., Volman, T.J., Kummer, J.A., 2010. The cytotoxic protease granzyme M is expressed by lymphocytes of both the innate and adaptive immune system. Mol. Immunol. 47, 903–911.

Ma, L.L., Spurrell, J.C., Wang, J.F., Neely, G.G., Epelman, S., Krensky, A.M., Mody, C.H., 2002. CD8 T cell-mediated killing of *Cryptococcus neoformans* requires granulysin and is dependent on CD4 T cells and IL-15. J. Immunol. 169, 5787–5795.

Rooney, M.S., Shukla, S.A., Wu, C.J., Getz, G., Hacohen, N., 2015. Molecular and genetic properties of tumors associated with local immune cytolytic activity. Cell 160, 48–61.

Sauce, D., Almeida, J.R., Larsen, M., Haro, L., Autran, B., Freeman, G.J., Appay, V., 2007. PD-1 expression on human CD8 T cells depends on both state of differentiation and activation status. AIDS 21, 2005–2013.

Spitzer, M.H., Nolan, G.P., 2016. Mass cytometry: single cells, many features. Cell 165, 780–791.

Stenger, S., Hanson, D.A., Teitelbaum, R., Dewan, P., Niazi, K.R., Froelich, C.J., Ganz, T., Thoma-Uszynski, S., Melian, A., Bogdan, C., Porcelli, S.A., Bloom, B.R., Krensky, A.M., Modlin, R.L., 1998. An antimicrobial activity of cytolytic T cells mediated by granulysin. Science 282, 121–125.

Voskoboinik, I., Whisstock, J.C., Trapani, J.A., 2015. Perforin and granzymes: function, dysfunction and human pathology. Nat. Rev. Immunol. 15, 388–400.
Walch, M., Dotiwala, F., Mulik, S., Thiery, J., Kirchhausen, T., Clayberger, C., Krensky, A.M., Martinvalet, D., Lieberman, J., 2014. Cytotoxic cells kill intracellular bacteria through granulysin-mediated delivery of granzymes. Cell 157, 1309–1323.
Wensink, A.C., Hack, C.E., Bovenschen, N., 2015. Granzymes regulate proinflammatory cytokine responses. J. Immunol. 194, 491–497.
Yu, J., Freud, A.G., Caligiuri, M.A., 2013. Location and cellular stages of natural killer cell development. Trends Immunol. 34, 573–582.
Zhang, D., Shankar, P., Xu, Z., Harnisch, B., Chen, G., Lange, C., Lee, S.J., Valdez, H., Lederman, M.M., Lieberman, J., 2003. Most antiviral CD8 T cells during chronic viral infection do not express high levels of perforin and are not directly cytotoxic. Blood 101, 226–235.